

group, the character associated with a translation  $\{\epsilon|\mathbf{R}_n\}$  is

$$d_{m,s} \sum_{j=1}^{n_s} \exp(i\mathbf{k}_j \cdot \mathbf{R}_n), \quad (\text{A4})$$

where  $d_{m,s}$  is the dimension of the  $m$ th irreducible representation of the group of the wave vector  $\mathbf{k}$ . From Eqs. (A3) and (A4), and the theorem quoted above, the number of times the  $m$ th irreducible representation of the space group associated with the star  $s$  is contained in the reducible representation is then

$$\begin{aligned} c_{m,s} &= (1/gN) \sum (R_n) \sum_{i,j=1}^{n_s} d_{m,s} g \exp[i(\mathbf{k}_j - \mathbf{k}_i) \cdot \mathbf{R}_n] \\ &= (1/gN) \sum_{i,j=1}^{n_s} d_{m,s} g N \delta_{ij} \\ &= d_{m,s} n_s. \end{aligned} \quad (\text{A5})$$

We now use the fact that the  $gn_s$  basis functions in

the reduction of the reducible representation must be made up out of sets of  $n_s d_{m,s}$  functions for the various irreducible representations of the space group; the dimensionality of such an irreducible representation equals the product of  $d_{m,s}$ , the dimensionality of the group of the wave vector, and  $n_s$ , the number of wave vectors in the star. We have seen in Eq. (A5) that we have  $c_{m,s}$  different sets of basis functions for the  $m$ th irreducible representation. We then have that

$$gn_s = \sum (m) c_{m,s} n_s d_{m,s} = \sum (m) (d_{m,s} n_s)^2. \quad (\text{A6})$$

This is what we set out to prove. As a simple corollary, we see that

$$(g/n_s) = \sum (m) (d_{m,s})^2. \quad (\text{A7})$$

Here  $(g/n_s)$  is the order of the point group associated with the wave vector  $\mathbf{k}$ . In words: the sum of the squares of the dimensionalities of the irreducible representations of the group of the wave vector equals the order of the point group of the group of the wave vector.

## Effects of Spin-Orbit Coupling in Si and Ge\*†

L. LIU†

*Department of Physics and Institute for the Study of Metals, University of Chicago, Chicago, Illinois,  
and Argonne National Laboratory, Argonne, Illinois*

(Received December 18, 1961)

A treatment of spin-orbit effects in some semiconductors is given using the effective-mass method and orthogonalized-plane-wave type wave functions. In this formalism, the spin-orbit splitting of valence states in the crystal is expressed directly in terms of either experimental or calculated values of the spin-orbit splitting of the atomic-core states. The calculation yields values in good agreement with experiments for the splitting at  $\Gamma_{25'}$  for Si and at both  $\Gamma_{25'}$  and  $L_3$  for Ge. A demonstration is given of the enhancement of the spin-orbit splitting of valence states in the crystal over the corresponding atomic value.

The shift in the  $g$  tensor due to spin-orbit interactions is studied in Si and Ge. Because of crystal selection rules, the usual two-band

approximation to the effective-mass sum rule is inadequate for Si and, in particular, the core state must be considered. When all important states are included, the calculations yield values in good agreement with experiment. In the case of Ge, it is found that core states do not contribute appreciably to the  $g$  tensor. However, the calculated value for the shift in the transverse component of the  $g$  tensor has an opposite sign to the measured one.

A certain matrix element of the deformation potential for Si is also evaluated based on the measured shift in the  $g$  value due to strain. The result is compared with other deformation potentials in Si.

### I. INTRODUCTION

THE effects of spin-orbit (s-o) coupling on the electronic properties of crystals have been discussed by several authors.<sup>1-6</sup> For semiconductors, these

properties are largely determined by the nature of the conduction and valence band edges. In semiconductors where these band edges are of  $p$  atomic symmetry and split under the s-o interaction, knowledge of the magnitude of their s-o splittings becomes necessary in any quantitative calculations. Although there have been recently several direct measurements of the valence state s-o splitting for<sup>7</sup> Si and<sup>8</sup> Ge by optical experiments, there is lack of any quantitative estimate in theory. In this work we attempt to estimate the s-o

\* A thesis submitted to the Department of Physics, the University of Chicago, in partial fulfillment of the requirements for the Ph.D. degree.

† Based on work performed under the auspices of the U.S. Atomic Energy Commission and supported in part by the Office of Naval Research and the National Science Foundation.

‡ Now at the Department of Physics, Northwestern University, Evanston, Illinois.

<sup>1</sup> R. J. Elliott, Phys. Rev. **96**, 266, 280 (1954).

<sup>2</sup> Y. Yafet, Phys. Rev. **85**, 478 (1952).

<sup>3</sup> L. M. Roth, B. Lax, and S. Zwerdling, Phys. Rev. **114**, 90 (1959).

<sup>4</sup> L. M. Roth, Phys. Rev. **118**, 1534 (1960).

<sup>5</sup> M. H. Cohen and E. I. Blount, Phil. Mag. **5**, 115 (1960).

<sup>6</sup> M. H. Cohen and L. M. Falicov, Phys. Rev. Letters **5**, 544 (1960).

<sup>7</sup> S. Zwerdling, K. J. Button, B. Lax, and L. M. Roth, Phys. Rev. Letters **4**, 173 (1960).

<sup>8</sup> A. H. Kahn, Phys. Rev. **97**, 1647 (1955); M. Cardona and H. S. Sommers, *ibid.* **122**, 1382 (1961); J. Tauc and A. Abraham, *Proceedings of the International Conference on Semiconductor Physics, Prague, 1960* (Czechoslovakian Academy of Sciences, Prague, 1961).

splitting of valence states in crystals by treating the s-o interaction as a perturbation on the crystal states described by orthogonalized-plane-wave (OPW) type wave functions, which are well suited to most semiconductors. But prior to this calculation, we treat the s-o splitting of the atomic-valence state using an atomic valence wave function, which, just like an OPW crystal wave function, consists of a smooth part plus occupied core orbitals. In this way, we can make a comparison between the splitting in the atom and that in the crystal and then demonstrate why the splitting gets enhanced in the crystal. Since both the atomic-valence wave function which we use and the OPW crystal wave function contain core orbitals, the s-o splitting of valence states in the atom and in the crystal can be expressed in terms of the s-o splitting of the atomic-core states in our formalism. We apply the splitting calculations to crystalline Si and Ge and obtain values in good agreement with experiment.

The effect of s-o interaction on the magnetic resonance is first of all a shift in the isotropic  $g$  value for conduction (or valence) electrons from the free electron value of 2.0023. Furthermore, when for some semiconductors like Si and Ge the conduction band edge consists of several valleys lying in equivalent positions along certain symmetry directions in the Brillouin zone (B.Z.), the s-o interaction introduces an anisotropy into the single-valley  $g$  value, which can be expressed as a tensorial quantity. Theoretical treatment of the  $g$  tensor for semiconductors or semimetals has been done in the framework of the effective mass approximation. In the absence of crystal wave functions, a two-level approximation to the effective-mass sum rule was further assumed to evaluate the  $g$  tensor for certain materials.<sup>3-5</sup> In other words, for semiconductors, it was assumed that the major contribution to the  $g$  shift for conduction (valence) electrons came from the s-o splitting of the nearest valence (conduction) level. In this way Roth has obtained excellent quantitative agreement with experiment for the longitudinal  $g$  shift in Ge<sup>4</sup> and the isotropic  $g$  value for InSb.<sup>3</sup> However, the two-level approximation is not always adequate. A typical semiconductor which illustrates this failure is Si. The Si valence s-o splitting at the conduction edge is very small due to special selection rules, and consequently, its contribution to the conduction  $g$  tensor is by no means dominating. Therefore, we attempt to do a more careful analysis. We still work with the effective mass approximation in evaluating the  $g$  tensor, but we use OPW crystal wave functions to calculate all the matrix elements involved in the effective-mass formalism. With the exception of the transverse component of the  $g$  tensor in Ge, excellent agreement with experiment is achieved. Since effective-mass parameters are involved in the  $g$  tensor calculation, we also include a section to discuss their evaluation from OPW wave functions.

The spin resonance linewidth in semiconductors is

largely due to a spin-lattice relaxation. Roth<sup>9</sup> has proposed a spin-lattice relaxation mechanism for Si, which is caused by the modulation of the single valley  $g$  tensor by strain. Using the measured value for a parameter in the proposed mechanism, we evaluate a certain shear deformation-potential matrix element. The result is compared with another deformation-potential matrix element obtained either from conductivity measurement or from measurement of spin-lattice relaxation rate due to a second mechanism proposed by Roth<sup>4</sup> and by Hasegawa<sup>10</sup> independently.

Part of the work on Si has been reported elsewhere.<sup>11</sup>

## II. SPIN-ORBIT SPLITTING OF ATOMIC STATES

It is our aim to treat in this section the s-o splitting of atomic valence states in a formalism related to the method we adopt later for the crystals so that we can see how the s-o splitting of energy levels differs in the atom and in the crystal.

The atomic s-o splitting is characterized by a matrix element

$$\langle n, j, l | \mathcal{H}_{s-o} | n, j, l \rangle = \xi_{nl} \langle \mathbf{l} \cdot \mathbf{s} \rangle_{j, l} \quad (2.1)$$

with

$$\xi_{nl} = \frac{1}{2m^2c^2} \int_0^\infty P_{nl}^2 \frac{1}{r} \frac{dV}{dr} dr, \quad (2.2)$$

where  $P_{nl}/r$  is the radial wave function for the state specified by quantum number  $n$ ,  $j$ , and  $l$ . With the tabulated atomic H-F wave functions we can evaluate numerically the one electron s-o coupling strength in (2.2). However, the valence radial wave function  $P_{nl}$  can also be represented by a smooth function which is orthogonalized to all the occupied core states with the same symmetry:

$$P_{nl} = N \left[ \left( \frac{(2a)^{2n'+1}}{(2n')!} \right)^{\frac{1}{2}} r^{n'} e^{-ar} - \sum_t B_t P_{tl} \right], \quad (2.3)$$

where  $N$  is a normalization factor and  $n'$  and  $a$  are two adjustable parameters. The coefficients  $B_t$  can be determined by the requirement that  $P_{nl}$  be orthogonal to the core states. In the core region, the wave function  $P_{nl}$  in (2.3) is dominated by its core terms, so we can neglect the smooth part for the s-o calculation. Then the s-o splitting  $\Delta_{nl}$  of the one electron valence state can be expressed in terms of that of the core states as

$$\Delta_{nl} = N^2 \sum_t B_t^2 \Delta_{tl} + N^2 \sum_{t, t'} B_t B_{t'} \langle \mathbf{l} \cdot \mathbf{s} \rangle_{j=t+\frac{1}{2}, l} - \langle \mathbf{l} \cdot \mathbf{s} \rangle_{j'=l-\frac{1}{2}, l} \frac{1}{(2m^2c^2)} \int_0^\infty P_{tl} P_{t'l} \frac{1}{r} \frac{dV}{dr} dr. \quad (2.4)$$

The second term is usually smaller than the first one.

<sup>9</sup> L. M. Roth, Lincoln Laboratory Reports, April, 1960 (unpublished), Vol. 15; *Proceedings of the International Conference on Semiconductor Physics, Prague, 1960* (Czechoslovakian Academy of Sciences, Prague, 1961).

<sup>10</sup> H. Hasegawa, Phys. Rev. **118**, 1523 (1960).

<sup>11</sup> L. Liu, Phys. Rev. Letters **6**, 683 (1961).

TABLE I. Core state spin-orbit splitting, in ev.

		Si	Ge
2 <i>p</i>	Exp.	0.72	31
	Corr. exp.	0.60	27
	Calc.	0.52	30
3 <i>p</i>	Calc.	...	4.0
3 <i>d</i>	Calc.	...	0.57

For neutral Ge, the atomic H-F wave functions have been calculated by Piper.<sup>12</sup> We use his wave functions for  $P_{nl}$  in (2.2) and also for constructing the atomic potential  $V$  assumed to be pure Coulombic to obtain the atomic s-o splitting for the various states. The calculated splittings for the core states are listed in Table I together with the core splitting for Si. The calculated value for the 4*p* splitting  $\Delta_{4p}$  in Ge is 0.15 ev. This is to be compared with the experimental value of  $\Delta_{4p}=0.18$  ev deduced from spectroscopic term values with a configuration of  $4s^2 4p^2 \ ^3P$ ,<sup>13</sup> the experimental value is about 20% greater than the calculated value.

On the other hand, we can fit Piper's wave function reasonably well by (2.3) with the following values for the parameters:

$$\begin{aligned} N &= 1.022, & B_{2p} &= 0.006520, \\ n' &= 4, & B_{3p} &= -0.1987, \\ a &= 1.85, \end{aligned} \quad (2.5)$$

Then, from (2.4), (2.5) and core splittings in Table I we obtain  $\Delta_{4p}=0.15$  ev, which is exactly the value obtained directly from the tabulated 4*p* function.

In our later discussion of the crystal case, we shall compare the crystal result with the atomic result obtained by (2.4). Through this explicit comparison we hope to illustrate the enhancement of the s-o splitting above atomic values found experimentally in certain crystals.

### III. SPIN-ORBIT SPLITTING OF ENERGY BANDS

There are different methods for calculating crystal energy bands and eigenfunctions in practical cases, but by far the most successful method for getting valence state wave functions in semiconductors is the OPW method. The crystal valence wave functions in terms of OPW's may be separated into a "smooth" plane wave part and a core part similar to the atomic valence function (2.3)

$$\psi_{\mathbf{k}}^{\alpha} = \sum_{\mathbf{K}} a(|\mathbf{k}+\mathbf{K}|) |(\mathbf{k}+\mathbf{K})\rangle^{\alpha} + \sum_{\mathbf{d}} b_{\mathbf{k},\mathbf{d}}^{\alpha} |\phi_{\mathbf{k},\mathbf{d}}^{\alpha}\rangle. \quad (3.1)$$

Here  $\alpha$  is a symbol for the irreducible representation used to denote the symmetry of the wave function,  $\mathbf{k}$  is the wave vector and  $\mathbf{K}$  is the reciprocal lattice vector. Plane waves are expressed by  $|\mathbf{k}+\mathbf{K}\rangle$ . The symbol

<sup>12</sup> W. W. Piper (to be published).

<sup>13</sup> C. E. Moore, *Atomic Energy Levels*, National Bureau of Standards Circular No. 467 (U. S. Government Printing Office, Washington, D. C., 1949).

$|\rangle^{\alpha}$  denotes a properly normalized symmetrized combination of plane waves. The second term in (3.1) is the core part, which comes from orthogonalization and takes the following form

$$\phi_{\mathbf{k},\mathbf{d}}^{\alpha} = \frac{1}{(sN)^{\frac{1}{2}}} \sum_{\mathbf{R}_n} \sum_{\mathbf{d}} \exp[i\mathbf{k} \cdot (\mathbf{R}_n + \mathbf{d})] \times \chi_t^{\alpha}(\mathbf{r} - \mathbf{R}_n - \mathbf{d}). \quad (3.2)$$

Here  $\chi_t^{\alpha}$  is the atomic-core wave function with symmetry specified by  $\alpha$ ,  $\mathbf{d}$  is the position of the atom with respect to the lattice vector  $\mathbf{R}_n$ ,  $N$  in the normalization factor is the number of unit cells in the crystal and  $s$  denotes the number of atoms per unit cell. The normalization of the wave function is such that both  $\chi_t^{\alpha}$  and  $\psi_{\mathbf{k}}^{\alpha}$  are normalized to one over the whole crystal.

For some semiconductors, the s-o coupling strength is small compared to the energy gap. In this case, the s-o Hamiltonian,  $\mathcal{H}_{s-o} = (\hbar/4m^2c^2)(\nabla V \times \mathbf{p}) \cdot \boldsymbol{\sigma} \equiv \mathbf{h} \cdot \boldsymbol{\sigma}$ , can be treated as a perturbation term. Then in order to evaluate the energy band splitting, we must first take matrix elements of  $\mathcal{H}_{s-o}$  with respect to states  $|\psi_{\mathbf{k}}^{\alpha}|\pm\rangle$ , where  $|+\rangle$  and  $|-\rangle$  are the two spin eigenstates of  $\sigma_z$ . A s-o matrix element using  $\psi_{\mathbf{k}}^{\alpha}$  in (3.1) can be separated into three parts; namely, the matrix element between two plane wave parts, between a plane wave part and a core part, and between two core parts. The last one gives the most important contribution. For example, in Si the core-core term is found to be about 96% of the whole matrix element. In Ge, because it has a larger core, the core-core term is even more important. Therefore, for the purpose of evaluating the s-o matrix element, we represent the valence wave function by its core part only. In this way a general matrix element of  $\mathcal{H}_{s-o}$  takes the following form:

$$\langle \psi_{\mathbf{k}}^{\alpha} \pm | \mathcal{H}_{s-o} | \psi_{\mathbf{k}}^{\beta} \pm \rangle \propto \sum_{t,t'} b_{\mathbf{k},t}^{\alpha*} b_{\mathbf{k},t'}^{\beta} \langle \chi_t^{\alpha} | h_i | \chi_{t'}^{\beta} \rangle. \quad (3.3)$$

To obtain the right-hand side of the above equation we have assumed that there is no overlap between the core orbitals centered around different lattice points. The operator  $h_i$  in  $\langle \chi_t^{\alpha} | h_i | \chi_{t'}^{\beta} \rangle$  is used to denote a definite component of  $\mathbf{h}$  determined by the symmetry  $\alpha$  and  $\beta$ .

We notice that the matrix element  $\langle \chi_t^{\alpha} | h_i | \chi_{t'}^{\beta} \rangle$  is connected with the s-o splitting of the core states. Therefore, the s-o splitting of the crystal valence states like that of the atomic valence state, can be expressed in terms of the splitting of all the occupied core states, the magnitude of which can be obtained either from x-ray data or from calculation using a model crystal potential and tabulated atomic wave functions. The coefficients  $b_{\mathbf{k},t}^{\alpha}$  can be expressed in terms of the plane wave coefficients  $a(|\mathbf{k}+\mathbf{K}|)$  in (3.1) and the orthogonalization coefficients  $B_t(\mathbf{k}+\mathbf{K})$  used in the usual OPW band calculation,

$$b_{\mathbf{k},t}^{\alpha} = -\sum_{\mathbf{K}} a(|\mathbf{k}+\mathbf{K}|) B_t(\mathbf{k}+\mathbf{K}) \exp(i\mathbf{K} \cdot \mathbf{d}), \quad (3.4)$$

where  $\alpha$  in the summation sign indicates that this is a symmetrized sum for  $\alpha$  irreducible representation. From (3.4) it is seen that the magnitude of  $(b_{k,l}^\alpha)^* b_{k,l'}^\beta$  in (3.3) depends on the number of terms we take in the expansion into symmetrized combination of OPW's for the valence wave functions. Any truncation of the infinite secular determinants arising in the OPW method not only leads to unavoidable errors to the energy eigenvalues but also to larger errors in the s-o splitting. Therefore in any calculation of the s-o splitting, it is advisable to study the convergence.

In order to illustrate the general procedures outlined above and to make explicit use of the crystal symmetry we take up in the following section diamond-type crystals.

#### IV. DIAMOND-TYPE CRYSTALS

There have been extensive studies on the energy bands for crystals with diamond structure. In particular, the band structures without s-o coupling for Si and Ge are sketched in Fig. 1 and Fig. 2, respectively. For both substances, the valence edge is at  $\Gamma_{25'}$ . The conduction edge for Si lies at  $\mathbf{k}_0 = (\Delta, 0, 0)$  along  $\Delta_1$  with  $\Delta = 0.85(2\pi/a)$ ,<sup>14</sup> and that for Ge lies at  $L_1$ . For these substances,  $\mathcal{H}_{s-o}$  can be treated as a perturbation term. Therefore, using the method outlined in the above section, we try to evaluate the splitting of the valence states at positions in the B.Z. corresponding to both the valence edge and to the conduction edge, or at  $\Gamma_{25'}$  and  $\Delta_5$  for Si and  $\Gamma_{25'}$  and  $L_{3'}$  for Ge.

The diamond structure consists of two interpenetrating face-centered cubic sublattices. We take as the origin of our coordinate system a point midway between two adjacent lattice points and distinguish the core orbitals in (3.2) centered around the two sublattices by a superscript 1 or 2 and denote the valence wave function by its core part only. In accordance with these

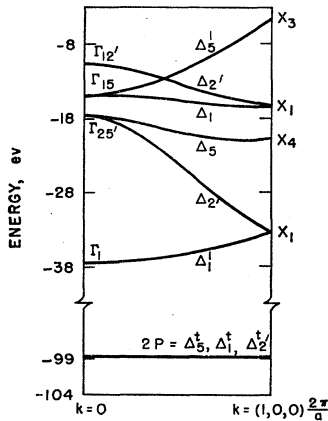


FIG. 1. Sketch of energy bands of Si along [100] axis of the Brillouin zone, after Kleinman and Phillips. Superscript  $i$  is used to denote the  $2p$  core states.

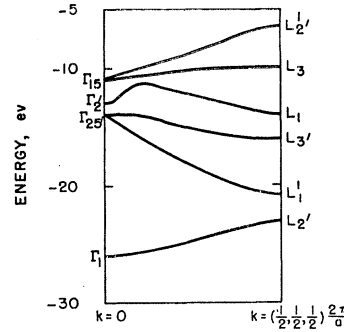


FIG. 2. Sketch of the energy bands of Ge along [111] axis of the Brillouin zone, after our own band calculation. The positions of  $\Gamma_{25'}$  and  $L_1$  states have been adjusted to fit the experimentally observed gap values. The core states are not shown.

conventions we list the wave functions  $\Gamma_{25'}$  and  $\Delta_5$ :

$$\Gamma_{25'}^{xy} = b_{2p} \Gamma_{25'}^{xy} (\phi_{2z}^1 - \phi_{2z}^2) + b_{3p} \Gamma_{25'}^{xy} (\phi_{3z}^1 - \phi_{3z}^2) + b_{3d} \Gamma_{25'}^{xy} (\phi_{xy}^1 + \phi_{xy}^2), \quad (4.1)$$

$$\Delta_5^{yz} = b_{2p} \Delta_5^{yz} (\phi_{2z}^1 - \phi_{2z}^2) + b_{2p} \Delta_5^{yz} (\phi_{2y}^1 + \phi_{2y}^2) + b_{3p} \Delta_5^{yz} (\phi_{3z}^1 - \phi_{3z}^2) + b_{3p} \Delta_5^{yz} (\phi_{3y}^1 + \phi_{3y}^2) + b_{3d} \Delta_5^{yz} (\phi_{xz}^1 - \phi_{xz}^2) + b_{3d} \Delta_5^{yz} (\phi_{yx}^1 + \phi_{yx}^2). \quad (4.2)$$

We have used the irreducible representation symbols to denote the wave functions with superscripts specifying the symmetry type. It is to be noted that we have only included core states up to the atomic  $3d$  state.

#### At $\Gamma_{25'}$

The valence state  $\Gamma_{25'}$  is sixfold degenerate (spin degeneracy included). When we treat  $\mathcal{H}_{s-o}$  by perturbation theory, we only take into consideration the three degenerate orbital states, one of which is given explicitly in (4.1), and the two spin eigenstates  $|+\rangle$  and  $|-\rangle$  of  $\sigma_z$ . With respect to these states, the only non-vanishing matrix elements of  $\mathcal{H}_{s-o}$  are:

$$\begin{aligned} \langle \Gamma_{25'}^{xy} \pm | \mathcal{H}_{s-o} | \Gamma_{25'}^{yz} \mp \rangle \\ = \mp i \{ |b_{2p} \Gamma_{25'}^{xy}|^2 \langle \chi_{2z} | h_y | \chi_{2z} \rangle + |b_{3p} \Gamma_{25'}^{xy}|^2 \langle \chi_{3z} | h_y | \chi_{3z} \rangle \\ + 2[\text{Re}(b_{2p} \Gamma_{25'}^{xy})^* b_{3p} \Gamma_{25'}^{xy}] \langle \chi_{2z} | h_y | \chi_{3z} \rangle \\ - |b_{3d} \Gamma_{25'}^{xy}|^2 \langle \chi_{yz} | h_y | \chi_{xy} \rangle \} \equiv \mp iS, \end{aligned} \quad (4.3)$$

$\langle \Gamma_{25'}^{xy} \pm | \mathcal{H}_{s-o} | \Gamma_{25'}^{zx} \mp \rangle$ , and  $\langle \Gamma_{25'}^{yz} \pm | \mathcal{H}_{s-o} | \Gamma_{25'}^{zx} \pm \rangle$  together with their complex conjugates. The  $6 \times 6$  Hamiltonian can be reduced to two identical  $3 \times 3$  matrices. In other words, the s-o split levels are at least doubly degenerate (Kramer's degeneracy). After diagonalization of the Hamiltonian, we see that the  $\Gamma_{25'}$  state splits into two, for which the energy shifts are

$$\Delta E_1 = iS \quad (\text{quartic degenerate}),$$

and

$$\Delta E_2 = -2iS \quad (\text{doubly degenerate}). \quad (4.4)$$

Since most of the s-o matrix elements in  $S$  are connected with the atomic core s-o splittings, the valence s-o splitting in the crystal can be conveniently obtained through the splitting of the core states  $\Delta_{2p}$ ,  $\Delta_{3p}$ , and

<sup>14</sup> J. C. Phillips, Phys. Rev. **112**, 685 (1958).

$\Delta_{3d}$  as follows:

$$\Delta_{s-o}(\Gamma_{25'}) = |b_{2p}^{\Gamma_{25'}}|^2 \Delta_{2p} + |b_{3p}^{\Gamma_{25'}}|^2 \Delta_{3p} - \frac{3}{5} |b_{3d}^{\Gamma_{25'}}|^2 \Delta_{3d} + 6[\text{Re}(b_{2p}^{\Gamma_{25'}})^* b_{3p}^{\Gamma_{25'}}](\chi_{2z}|\chi_{3z}). \quad (4.5)$$

According to (3.4), the coefficient  $b$ 's in terms of plane-wave and orthogonalization coefficients are equal to

$$b_{2p,3p}^{\Gamma_{25'}} = i[(2/\sqrt{3})a(\sqrt{3})B_{2p,3p}(\sqrt{3}) + \sqrt{2}a(2)B_{2p,3p}(2) + \dots], \quad (4.6)$$

$$b_{3d}^{\Gamma_{25'}} = (2/\sqrt{3})a(\sqrt{3})B_{3d}(\sqrt{3}) + \sqrt{3}a(2\sqrt{2})B_{3d}(2\sqrt{2}) + \dots.$$

Here we have used orthogonalization coefficients which depend only on the magnitude  $|\mathbf{k}+\mathbf{K}|$  of the wave vectors, given in units of  $2\pi/a$  in the argument of both  $a$  and  $B_i$ . The variation of  $B_i(\mathbf{k}+\mathbf{K})$  with the directions of a set of wave vectors of the same magnitude has been absorbed into the numerical factors in (4.6).

In any quantitative evaluation of the splitting of  $\Gamma_{25'}$  according to (4.5), we first need the splitting of the core states. This can be obtained either from experimental x-ray data or from calculation. On the experimental side, Tomboulia and Cady<sup>15</sup> have completed the identification of the x-ray emission lines  $2p^3 \rightarrow 2s$  and  $2p^3 \rightarrow 2s$  for the second row of the periodic table. Their value for the  $2p$  s-o splitting of Si is listed in the first line of Table I. By invoking Slater's rule that the missing electron gives an extra screening charge of 0.3 ev, we can use Tomboulia and Cady's values to estimate the  $2p$  splitting in neutral Si (second line of Table I). As for Ge, there is only an experimental value for the  $2p$  core s-o splitting by Tyren<sup>16</sup> from K-emission data. This value and the corrected value for neutral Ge are also listed.

On the other hand, to calculate the core s-o splitting we assume that the crystal potential has spherical symmetry in the vicinity of each atomic site. We have already calculated the core splitting for Ge in Sec. II and we calculate now the  $2p$  core splitting for Si based on crystal potential and atomic core wave functions used by Kleinman and Phillips<sup>17</sup> in their Si band calculation. All the calculated results are listed in Table I. In all the subsequent calculations we shall use the corrected experimental value for the Si  $2p$  core s-o splitting and the calculated values for the three Ge core ( $2p$ ,  $3p$ , and  $3d$  states) splittings.

To obtain the plane-wave and orthogonalization coefficients for the evaluation of  $b_{2p,3p}^{\Gamma_{25'}}$  and  $b_{3d}^{\Gamma_{25'}}$  in (4.6) for Si, we rely upon K-P's crystal wave functions. For Ge, we use the H-F atomic wave function by Piper<sup>12</sup> and a computer program furnished by Bassani and Yoshimine to run the Ge OPW crystal

wave function on an IBM 704 computer. We include in the Appendix a brief discussion on this calculation and a list of the orthogonalization and plane-wave coefficients. The corresponding Si values may be obtained from K-P.

With the core splittings and coefficients  $b$  and  $b'$ , we evaluate the s-o splitting of the  $\Gamma_{25'}$  state for Si and Ge by successively taking more and more plane waves in (4.6). The convergence of the calculation is shown in Fig. 3. After about 80 plane waves the calculated splitting is expected to change by no more than 7%, because the plane-wave coefficients for any higher  $\mathbf{K}$  are very small. This expectation is represented by dashed lines in Fig. 3 indicating approximate convergence. In the study of convergence, we have neglected the contribution from  $2p-3p$  interference term in (4.5) to  $\Delta_{s-o}^{\text{Ge}}$ ; this is to be corrected in the final result. The s-o splittings for Ge and Si thus obtained are  $\Delta_{s-o}^{\text{Si}}(\Gamma_{25'}) = 0.042$  ev and  $\Delta_{s-o}^{\text{Ge}}(\Gamma_{25'}) = 0.29$  ev. They are to be compared with the experimental values of  $\Delta_{s-o}^{\text{Si}}(\Gamma_{25'}) = 0.0441 \pm 0.0004$  ev<sup>7</sup> and  $\Delta_{s-o}^{\text{Ge}}(\Gamma_{25'}) = 0.3$  ev.<sup>8</sup> The agreement in both cases is good. In the calculation for  $\Delta_{s-o}^{\text{Ge}}(\Gamma_{25'})$  we find that the  $3d$  state contributes only 2% (of opposite sign to the contribution from  $p$  states) and the  $2p$  state 4% to this value.

As  $\Gamma_{25'}$  is of atomic  $p$  symmetry type, we compare  $\Delta_{s-o}^{\text{Ge}}(\Gamma_{25'})$  with  $\Delta_{4p}^{\text{Ge}}$  of Sec. II. We notice that according to calculations the splitting in the crystal is about 2 times larger than that in the atom. To see how this enhancement comes about, we compare  $b_i^{\Gamma_{25'}}$  of (4.6) with  $NB_{2p}$  in (2.4). The average value of the orthogonalization coefficients  $B_i(|\mathbf{k}+\mathbf{K}|)$  in  $b_i^{\Gamma_{25'}}$  is about the same in magnitude as the corresponding  $B_i$  for the atomic wave function. However the rest of  $b_i^{\Gamma_{25'}}$ , which is essentially a summation of plane-wave coefficients, adds up to 1.78 for about 80 plane waves in (4.6) while in the atomic case  $N=1.02$ . Physically, this difference in normalization constants means that the wave function in crystal gets contracted in the core region of each atomic site. It is this contraction which gives rise to an enhancement of the s-o splitting. For Si, the same enhancement is noticed; the atomic splitting  $\Delta_{3p}^{\text{Si}} = 0.028$  ev from spectroscopic term values<sup>13</sup> with the configuration  $3s^2 3p^2 3P$ . Since at

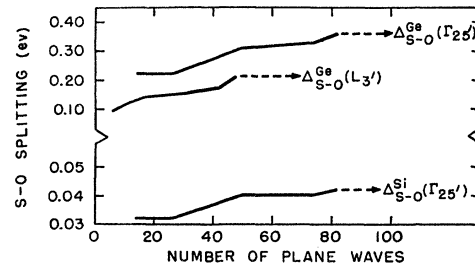


Fig. 3. Convergence of the calculated spin-orbit splitting values vs number of orthogonalized plane waves taken in the wave function. The dashed lines indicate expected convergence.

<sup>15</sup> D. H. Tomboulia and W. M. Cady, Phys. Rev. **59**, 422 (1944).

<sup>16</sup> F. Tyren, Arkiv. Mat. Astron. Fysik **A25**, Nr. 32 (1937).

<sup>17</sup> L. Kleinman and J. C. Phillips, Phys. Rev. **118**, 1153 (1960): Hereafter referred to as K-P.

present there are no atomic H-F wave functions calculated for neutral Si, it is not possible to carry out a calculation similar to what we did for Ge in Sec. II to demonstrate the enhancement.

### Along $\Delta_5$ for Si

The s-o splitting of the energy bands along  $\Delta_5$  in diamond structure solids has been qualitatively discussed by Englert.<sup>18</sup> Although he uses tight-binding-type wave functions while we use OPW crystal wave functions, the qualitative features of our results are the same since they all depend on the crystal symmetry only.

For simplicity, we consider explicitly the case for Si in this section. We first consider the region near the zone edge  $X_4$  and then the region near  $\Gamma_{25'}$ . In the former region, we are far away from the zone center. Then in studying the s-o splitting of the  $\Delta_5$  valence band, we only need take the two degenerate states  $\Delta_5^y$  and  $\Delta_5^z$  into consideration, one of which is given in (4.2). With respect to these states, the only non-vanishing matrix elements of  $\mathcal{H}_{s-o}$  are:

$$\langle \Delta_5^y \pm | \mathcal{H}_{s-o} | \Delta_5^z \rangle = (|b_{2p}'^{\Delta_5}|^2 - |b_{2p}^{\Delta_5}|^2) \langle \chi_{2y} | h_x | \chi_{2z} \rangle, \quad (4.7)$$

and their complex conjugates. Then, the degenerate  $\Delta_5$  state splits into two states, each doubly degenerate (Kramer's degeneracy), and the splitting is equal to

$$\Delta_{s-o}^{\text{Si}}(\Delta_5) = \frac{2}{3} | |b_{2p}'^{\Delta_5}|^2 - |b_{2p}^{\Delta_5}|^2 | \Delta_{2p}^{\text{Si}}. \quad (4.8)$$

In terms of parameters in OPW-type band calculations, the coefficients  $b_{2p}^{\Delta_5}$  and  $b_{2p}'^{\Delta_5}$  are:

$$\begin{aligned} b_{2p}^{\Delta_5} &= \sqrt{2}i \left\{ \frac{1}{(\delta^2+2)^{\frac{3}{2}}} a((\delta^2+2)^{\frac{1}{2}}) B_{2p}((\delta^2+2)^{\frac{1}{2}}) \right. \\ &\quad + \frac{2}{[(\delta+1)^2+4]^{\frac{3}{2}}} a[(\delta+1)^2+4]^{\frac{1}{2}} \\ &\quad \times B_{2p}[(\delta+1)^2+4]^{\frac{1}{2}} + \dots \left. \right\}, \\ b_{2p}'^{\Delta_5} &= -\sqrt{2} \left\{ \frac{1}{(\delta^2+2)^{\frac{3}{2}}} a((\delta^2+2)^{\frac{1}{2}}) B_{2p}((\delta^2+2)^{\frac{1}{2}}) \right. \\ &\quad + \frac{2}{[(\delta-1)^2+4]^{\frac{3}{2}}} a[(\delta-1)^2+4]^{\frac{1}{2}} \\ &\quad \times B_{2p}[(\delta-1)^2+4]^{\frac{1}{2}} + \dots \left. \right\}, \end{aligned} \quad (4.9)$$

using the direction independent orthogonalization coefficients as in (4.6). Here  $(\delta+1, 0, 0)$  is the position in the B.Z. under consideration in units of  $2\pi/a$ .

<sup>18</sup> F. Englert, Bull. classe sci., Acad. roy Belg. **43**, 273 (1957).  $\psi_z$  and  $\psi_y$  in Eqs. (5) and (6) of this paper should be interchanged. Also Eqs. (27)–(29) are in error.

According to the terms listed in (4.9), the difference in  $|b_{2p}^{\Delta_5}|$  and  $|b_{2p}'^{\Delta_5}|$  is due to one containing the  $(\delta+1, 2, 0)$  set of plane waves and the other the  $(\delta-1, 2, 0)$  set. The first thing to be noted is that at  $X_4(\delta=0)$ ,  $|b_{2p}^{\Delta_5}|$  is equal to  $|b_{2p}'^{\Delta_5}|$ . Then, according to (4.8)

$$\Delta_{s-o}^{\text{Si}}(X_4) = 0, \quad (4.10)$$

which is consistent with the prediction by Elliott<sup>1</sup> using the theory of the double group. Next, we go away from  $X_4$  toward the zone center but keep  $|\delta|$  small. By (4.8) and (4.9), the s-o splitting of the  $\Delta_5$  state reflects the properties of the wave functions through the difference between  $b_{2p}^{\Delta_5}$  and  $b_{2p}'^{\Delta_5}$ . However, the orthogonalization coefficients and the numerical factors in  $|b_{2p}^{\Delta_5}|$  and  $|b_{2p}'^{\Delta_5}|$  are not sensitive functions of  $k$ ; their product only changes about 1% when  $|\delta|$  changes from 0 to 0.5. Therefore, the difference is mainly due to the coefficients  $a(|\mathbf{k}+\mathbf{K}|)$ . The secular determinants for  $\Delta_5$  and  $X_4$  in the OPW method have identical off-diagonal elements; only their diagonal elements  $(\hbar^2/2m)(\mathbf{k}+\mathbf{K})^2$  differ. Therefore, by using perturbation technique, we can establish that

$$\begin{aligned} a^{\Delta_5}[(\delta+1)^2+4]^{\frac{1}{2}} &= a^{x_4}(\sqrt{5})(1+\frac{2}{3}|\delta|), \\ a^{\Delta_5}[(\delta-1)^2+4]^{\frac{1}{2}} &= a^{x_4}(\sqrt{5})(1-\frac{2}{3}|\delta|), \end{aligned} \quad (4.11)$$

when  $\delta$  is small. It is then evident from (4.8) that  $\Delta_{s-o}(\Delta_5)$  is proportional to  $|\delta|$  if higher order terms are neglected. To determine the proportionality constant, we calculate the s-o splitting of  $\Delta_5$  at the conduction band edge  $\mathbf{k}_0$  for Si ( $\delta=-0.15$  at  $\mathbf{k}_0$ ). The calculation using the band parameters of K-P establishes that

$$\Delta_{s-o}^{\text{Si}}(\Delta_5) = 0.17 |\delta| \Delta_{s-o}^{\text{Si}}(\Gamma_{25'}), \quad (\text{near } X_4) \quad (4.12)$$

where  $\delta$  is in units of  $2\pi/a$  as before.

We now go to the region in the vicinity of  $\mathbf{k}=0$ . First we would like to mention that although there is a splitting for  $\Gamma_{25'}$ , the lower doubly degenerate level goes to  $\Delta_7$  (in the notation of the double group) associated with the orbital state  $\Delta_2'$ . So, as far as the orbital state  $\Delta_5$  is concerned, the splitting is zero at the zone center. In the vicinity of  $\mathbf{k}=0$ , we have to take the  $\Delta_2'$  state into consideration when studying the s-o splitting of  $\Delta_5$ . The conduction state  $\Delta_1$  does not have much influence since the conduction-valence energy gap is about 30 times larger than the  $\Delta_5$  s-o splitting. Using the three states  $\Delta_5^y$ ,  $\Delta_5^z$ , and  $\Delta_2'$  as a basis, we diagonalize the s-o Hamiltonian and get the energy shift for the  $\Delta_5$  level as

$$\begin{aligned} \Delta_{s-o}^{\text{Si}}(\Delta_5) &= \frac{1}{2} | E_{\Delta_5} - E_{\Delta_2'} + \Delta_{s-o}^{\text{Si}}(\Gamma_{25'}) \\ &\quad - [(E_{\Delta_5} - E_{\Delta_2'} + \frac{1}{3} \Delta_{s-o}^{\text{Si}}(\Gamma_{25'}))^2 \\ &\quad + (8/9) \Delta_{s-o}^{\text{Si}^2}(\Gamma_{25'}) ]^{\frac{1}{2}}, \quad (\text{near } \Gamma_{25'}). \end{aligned} \quad (4.13)$$

In obtaining (4.13), we have assumed that all band parameters appropriate to small  $\mathbf{k}$  are given by those at  $\mathbf{k}=0$ . Furthermore, in the vicinity of  $\mathbf{k}=0$ ,  $E_{\Delta_5}$  and

$E_{\Delta_2'}$  are given in terms of hole effective-mass parameters<sup>19,20</sup> so that

$$E_{\Delta_5}(k) - E_{\Delta_2'}(k) = (M - L)k^2. \quad (4.14)$$

The values of  $M$  and  $L$  for Si as deduced from experiments<sup>17,21</sup> are  $M = -6.1$  and  $L = -2.8$  in units of  $\hbar^2/2m$ . Therefore, we can use (4.13) to get a quantitative estimate of the s-o splitting for  $\Delta_5$  near the center of the B.Z.

In summary, we see that at the zone center, the s-o splitting for  $\Delta_5$  is equal to zero. As we move away from the center, the splitting increases and then decreases to zero again at the zone edge. A sketch of  $\Delta_{s-o}^{\text{Si}}(\Delta_5)$  vs  $k_x$  is given in Fig. 4.

#### At $L$ and Along $\Delta$ for Ge

To evaluate the s-o splitting at  $L_{3'}$  for Ge, we still treat  $\mathcal{H}_{s-o}$  as a perturbation on the doubly degenerate state  $L_{3'}$ , the wave function of which can be obtained in the same way as (4.1) or (4.2). The calculated results vs number of plane waves taken for the basis functions is again shown in Fig. 3. We take as our calculated result  $\Delta_{s-o}^{\text{Ge}}(L_{3'}) = 0.18$  ev after putting in correction due to  $2p-3p$  cross term. The most recent experimental value for a reflectivity measurement by Cardona and Sommers<sup>8</sup> is  $\Delta_{s-o}^{\text{Ge}}(L_{3'}) = 0.18$  ev. In the calculation we find again as in the case of  $\Delta_{s-o}^{\text{Ge}}(\Gamma_{25'})$  that the most important state which contributes to the s-o splitting of these valence states is the  $3p$  core state. The  $3d$  state contributes a value of less than 1% and  $2p$  a value of about 4% of the total splitting.

In a similar way we calculate  $\Delta_{s-o}^{\text{Ge}}(L_3)$  to be 0.01 ev, or much smaller in value than  $\Delta_{s-o}^{\text{Ge}}(L_{3'})$ . Also different from the case of  $L_{3'}$  is that  $L_3$  is predominantly of  $d$  character in the core region. Therefore, in the tight-binding language,  $L_3$  is a bonding  $4d$  state while  $L_{3'}$  is an antibonding  $4p$  state. This comes about because they are close in energy on the nearly free electron picture. The significance of the difference in bonding and antibonding s-o splittings has been discussed by Phillips and Liu.<sup>22</sup>

Next, we discuss qualitatively the behavior of the s-o splitting of  $\Delta_3$  in going from  $\Gamma_{25'}$  to  $L_{3'}$  along the  $[111]$  axis in the B.Z. By symmetry we see that  $\Gamma_{25'}$  contains bonding  $p$  character (antibonding  $d$  character), or  $\phi_p^1 - \phi_p^2$  type wave functions while  $L_{3'}$  contains antibonding  $p$  character (bonding  $d$  character), or  $\phi_p^1 + \phi_p^2$  type wave functions. Along  $\Delta_3$  there is no inversion symmetry in the group of the  $k$  vector; hence, both bonding and antibonding types are allowed in the

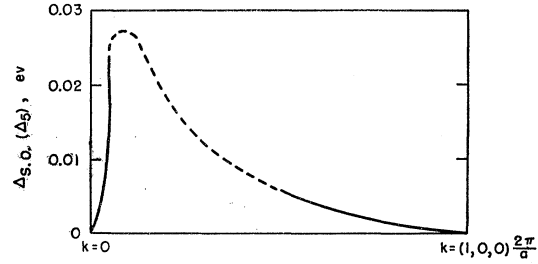


FIG. 4. Sketch of the spin-orbit splitting of the  $\Delta_5$  valence band of Si. The dashed curve represents interpolation from the calculated results.

wave function. Somewhere along  $\Delta_3$ , the weight of the two types must be equal. Then, according to procedures which lead to (4.8), the s-o splitting should vanish at this point. This shows that the s-o split levels along  $\Delta_3$  have a crossover. We shall see in Sec. V that under a two-band approximation the longitudinal  $g$  tensor for conduction electrons in Si is related to the s-o splitting of the  $\Delta_5$  valence state, and is larger than the free-electron  $g$  value 2.0023. When we go from  $\Delta_5$  to  $L_{3'}$ , we encounter a crossover in the s-o split levels. Since the s-o splitting at  $L_{3'}$  is related to the longitudinal  $g$  tensor for conduction electrons in Ge, it becomes smaller than 2.0023 under a two-level assumption, which is consistent with experiments.

#### V. $g$ TENSOR

As we have seen in the last section, there exists a Kramer's degeneracy in the energy bands of diamond-type crystals even with s-o interaction. However, if we put the crystals under a magnetic field of strength  $H$ , the twofold degeneracy is lifted. The Hamiltonian then has an additional term

$$\mathcal{H}_m = \frac{1}{2}\beta\sigma \cdot \mathbf{g} \cdot \mathbf{H}, \quad (5.1)$$

where  $\beta$  is the Bohr magneton. In the absence of s-o interaction,  $g$  becomes a scalar quantity and is equal to 2.0023. On the other hand, in addition to a diamagnetic contribution, the orbital motion of the electron under a magnetic field changes the value of  $g$  from 2.0023 through s-o coupling. For some semiconductors when the conduction band edges consist of several valleys and lie along symmetry axis instead of at the origin of the B.Z., the electron energy surface may no longer be a sphere even if the crystal possesses cubic symmetry. In this case, s-o interaction introduces anisotropy into the  $g$  value and makes it a tensorial quantity as indicated in (5.1). To obtain in theory the dependence of the tensor  $g$  on the details of the orbital motion of Bloch electrons is in general a difficult task because the magnetic interaction cannot be treated as a perturbation on Bloch states which have a quasi-continuous energy spectrum. For Na, Yafet<sup>2</sup> used a cellular method to solve numerically the magnetic

<sup>19</sup> G. Dresselhaus, A. F. Kip, and C. Kittel, Phys. Rev. **98**, 368 (1955).

<sup>20</sup> G. Dresselhaus, Ph.D. thesis, University of California, 1955 (unpublished).

<sup>21</sup> B. Lax, Revs. Modern Phys. **30**, 122 (1958).

<sup>22</sup> J. C. Phillips and L. Liu, Phys. Rev. Letters **8**, 94 (1962).

Schrödinger equation to obtain the  $g$  factor. For paramagnetic ions embedded in crystalline salts, we abandon the band picture and regard the electron as localized at the ion position. Then, with respect to the discrete atomic states, the electronic interaction with crystalline field and magnetic field can be treated by perturbation theory. This localized electron picture does not apply to conduction electrons in semiconductors. Nevertheless, since only states in the immediate vicinity of band edges are important, we can ignore the  $\mathbf{k}$  dependence of the  $g$  tensor and use the effective-mass approximation. In this approximation, general formula for the  $g$  tensor are contained in several papers<sup>4,5</sup> and need not be repeated here. For some semiconductors like Si and Ge, details of energy band structure are known and use can be made of the symmetry properties of various states to obtain selection rules for the matrix elements involved in the effective-mass formalism. In this way Roth derived the following formula for the  $g$  shift of conduction electrons in Si and Ge by treating  $\mathcal{H}_{s-o}$  as a perturbation.

$$\begin{aligned} \delta g_{11}^{\text{Si}} = \delta g_x^{\text{Si}} = & \text{Re} \frac{4}{mi_{\mu,\nu}} \frac{1}{E_{0\mu}E_{0\nu}} \langle \Delta_1 | p_y | \Delta_5^{\mu y} \rangle \\ & \times \langle \Delta_5^{\mu y} | h_x | \Delta_5^{\nu z} \rangle \langle \Delta_5^{\nu z} | p_z | \Delta_1 \rangle \\ & + \text{Re} \frac{8}{mi_{\mu,\nu}} \frac{1}{E_{0\mu}E_{0\nu}} \langle \Delta_1 | h_x | \Delta_1^{\mu} \rangle \\ & \times \langle \Delta_1^{\mu} | p_y | \Delta_5^{\nu z} \rangle \langle \Delta_5^{\nu z} | p_z | \Delta_1 \rangle, \\ \delta g_{11}^{\text{Si}} = \delta g_{y,z}^{\text{Si}} = & \text{Re} \frac{4}{mi_{\mu,\nu}} \frac{1}{E_{0\mu}E_{0\nu}} \langle \Delta_1 | p_z | \Delta_5^{\mu z} \rangle \\ & \times \langle \Delta_5^{\mu z} | h_y | \Delta_1^{\nu} \rangle \langle \Delta_1^{\nu} | p_x | \Delta_1 \rangle \\ & + \text{Re} \frac{4}{mi_{\mu,\nu}} \frac{1}{E_{0\mu}E_{0\nu}} \langle \Delta_1 | h_y | \Delta_5^{\mu z} \rangle \\ & \times \langle \Delta_5^{\mu z} | p_z | \Delta_1^{\nu} \rangle \langle \Delta_1^{\nu} | p_x | \Delta_1 \rangle \\ & + \text{Re} \frac{4}{mi_{\mu,\nu}} \frac{1}{E_{0\mu}E_{0\nu}} \langle \Delta_1 | p_z | \Delta_5^{\mu z} \rangle \\ & \times \langle \Delta_5^{\mu z} | p_x | \Delta_5^{\nu z} \rangle \langle \Delta_5^{\nu z} | h_y | \Delta_1 \rangle, \end{aligned} \quad (5.2)$$

and

$$\begin{aligned} \delta g_{11}^{\text{Ge}} = \delta g_{x'}^{\text{Ge}} = & \text{Re} \frac{4}{mi_{\mu,\nu}} \frac{1}{E_{0\mu}E_{0\nu}} \langle L_1 | p_{y'} | L_{3'}^{\mu y'} \rangle \\ & \times \langle L_{3'}^{\mu y'} | h_{x'} | L_{3'}^{\nu z'} \rangle \langle L_{3'}^{\nu z'} | p_{z'} | L_1 \rangle \\ & + \text{Re} \frac{8}{mi_{\mu,\nu}} \frac{1}{E_{0\mu}E_{0\nu}} \langle L_1 | h_{x'} | L_2^{\mu} \rangle \\ & \times \langle L_2^{\mu} | p_{y'} | L_{3'}^{\nu z'} \rangle \langle L_{3'}^{\nu z'} | p_{z'} | L_1 \rangle, \end{aligned}$$

$$\begin{aligned} \delta g_{11}^{\text{Ge}} = \delta g_{y',z'}^{\text{Ge}} = & \text{Re} \frac{4}{mi_{\mu,\nu}} \frac{1}{E_{0\mu}E_{0\nu}} \langle L_1 | p_{z'} | L_{3'}^{\mu z'} \rangle \\ & \times \langle L_{3'}^{\mu z'} | h_{y'} | L_{2'}^{\nu} \rangle \langle L_{2'}^{\nu} | p_{x'} | L_1 \rangle \\ & + \text{Re} \frac{4}{mi_{\mu,\nu}} \frac{1}{E_{0\mu}E_{0\nu}} \langle L_1 | h_{y'} | L_{3'}^{\mu z'} \rangle \\ & \times \langle L_{3'}^{\mu z'} | p_{z'} | L_{2'}^{\nu} \rangle \langle L_{2'}^{\nu} | p_{x'} | L_1 \rangle \\ & + \text{Re} \frac{4}{mi_{\mu,\nu}} \frac{1}{E_{0\mu}E_{0\nu}} \langle L_1 | p_{z'} | L_{3'}^{\mu z'} \rangle \\ & \times \langle L_{3'}^{\mu z'} | p_{x'} | L_{3'}^{\nu z'} \rangle \langle L_{3'}^{\nu z'} | h_y | L_1 \rangle. \end{aligned} \quad (5.3)$$

In (5.3), the primed coordinate  $x'$  is used to denote the [111] direction, which is the principal axis of the electron energy ellipsoid in Ge. The expression contains the linear momentum  $\mathbf{p}$  matrix elements from the effective-mass approximation and the matrix elements of  $\mathbf{h}$  from s-o coupling. See Figs. 1 and 2 for relevant energy levels. Note the core states with superscript “ $t$ .”

### Effective Mass

From the formula for the  $g$  tensor in the effective mass formalism like (5.2) or (5.3), we see that any calculation of the  $g$  tensor involves calculation of s-o and momentum matrix elements. Calculation of s-o matrix elements from OPW crystal wave functions has already been discussed. We now discuss the evaluation of electron effective mass with OPW-type wave functions, which involves the calculation of momentum matrix elements.

We rewrite the OPW function in a general form without explicitly specifying its symmetry

$$\psi_{\mathbf{k}} = \sum_{\mathbf{K}} a(\mathbf{k}+\mathbf{K}) \left[ \frac{1}{\sqrt{V}} e^{i(\mathbf{k}+\mathbf{K}) \cdot \mathbf{r}} - \sum_t B_t(\mathbf{k}+\mathbf{K}) \phi_{t,\mathbf{k}+\mathbf{K}} \right], \quad (5.4)$$

where  $\phi_{t,\mathbf{k}+\mathbf{K}}$  is defined similar to  $\phi_{t,\mathbf{k}^\alpha}$  in (3.2) and the normalization is such that the plane-wave part of  $\psi_{\mathbf{k}}$  is normalized to 1 over the whole space. The momentum matrix element is then evaluated.

$$\begin{aligned} \langle \psi_{\mathbf{k}} | \mathbf{p} | \psi_{\mathbf{k}} \rangle / \langle \psi_{\mathbf{k}} | \psi_{\mathbf{k}} \rangle = & \frac{1}{\langle \psi_{\mathbf{k}} | \psi_{\mathbf{k}} \rangle} \sum_{\mathbf{K}, \mathbf{K}'} a^*(\mathbf{k}+\mathbf{K}) a(\mathbf{k}+\mathbf{K}') \\ & \times \{ \hbar(\mathbf{k}+\mathbf{K}) [\delta_{\mathbf{K}, \mathbf{K}'} - 2 \sum_t B_t^*(\mathbf{k}+\mathbf{K}) B_t(\mathbf{k}+\mathbf{K}')] \\ & + \sum_{t, t'} B_t^*(\mathbf{k}+\mathbf{K}) B_{t'}(\mathbf{k}+\mathbf{K}') \langle \chi_t | \mathbf{p} | \chi_{t'} \rangle \}, \end{aligned} \quad (5.5)$$

where

$$\begin{aligned} \langle \psi_{\mathbf{k}} | \psi_{\mathbf{k}} \rangle = & \sum_{\mathbf{K}, \mathbf{K}'} a(\mathbf{k}+\mathbf{K})^* a(\mathbf{k}+\mathbf{K}') \\ & \times [\delta_{\mathbf{K}, \mathbf{K}'} - \sum_t B_t^*(\mathbf{k}+\mathbf{K}) B_t(\mathbf{k}+\mathbf{K}')]. \end{aligned} \quad (5.6)$$

Since absolute square of the orthogonalization coefficients is small compared with 1, the last two terms in (5.5) are normally negligible. In addition, the normalization factor in (5.6) may counterbalance the two additional factors due to the core orbitals depending on the sign and the magnitude of the momentum matrix element  $\langle \chi_t | \mathbf{p} | \chi_t' \rangle$ . This cancellation has been found by K-P in their calculation of the electron and hole-effective mass for Si.<sup>17</sup> In a similar calculation for Ge in this section, we hope that this cancellation still prevails. Therefore, we shall take the plane-wave part only for the OPW wave function and at the same time neglect the core contribution to the normalization factor.

The two components of electron effective mass in Ge are given by

$$\left(\frac{m}{m_i^*}\right)_{\text{Ge}} = 1 + \frac{2}{m} \sum_{\mu} \frac{1}{E_{0\mu}} |\langle L_1 | p_{y'} | L_{3'}^{\mu y'} \rangle|^2, \quad (5.7)$$

$$\left(\frac{m}{m_i^*}\right)_{\text{Ge}} = 1 + \frac{2}{m} \sum_{\mu} \frac{1}{E_{0\mu}} |\langle L_1 | p_{x'} | L_{2'}^{\mu x'} \rangle|^2.$$

A two-level approximation is sufficient for the evaluation of (5.7). For  $m/m_i^*$  the relevant two levels are the conduction band  $L_1$  and the valence band  $L_{3'}$ ; for  $m/m_i^*$  they are  $L_1$  and  $L_{2'}$ , which lies above the conduction band in energy. By using the experimental energy gap value<sup>23</sup>  $E_{L_1} - E_{L_{3'}} = 2.1$  eV<sup>24</sup> for  $m/m_i^*$  and our calculated gap value  $E_{L_1} - E_{L_{2'}} = -4.8$  eV for  $m/m_i^*$ , the effective-mass components are found to be  $(m/m_i^*)_{\text{Ge}} = 12$  and  $(m/m_i^*)_{\text{Ge}} = 0.52$ . Comparing these with the experimental values<sup>24</sup> of  $(m/m_i^*)_{\text{Ge}} = 12$  and  $(m/m_i^*)_{\text{Ge}} = 0.61$  from cyclotron resonance, we see that the agreement is satisfactory. Our calculated value  $-4.8$  eV for  $E_{L_1} - E_{L_{2'}}$  is probably too small in magnitude. A better energy gap value may improve the agreement in the case of  $(m/m_i^*)_{\text{Ge}}$ .

Phillips,<sup>14</sup> using the crystal wave function for Ge obtained by his interpolation scheme, evaluated  $(m/m_i^*)_{\text{Ge}}$  to be 6.7, or only about one half of the experimental value. It is suspected that this is due to a computational mistake rather than usage of an incorrect value for the energy gap as conjectured by Phillips in his paper.

The Ge hole effective-mass parameters have not been calculated here because we are not going to consider the  $g$  factor for holes in this work. The calculation of electron and hole effective-mass tensor components for Si has been done by K-P.<sup>17</sup>

### Two-Band Approximation

From (5.2) and (5.3), we would think it natural that the s-o splitting of the nearby valence band should be

responsible for the shift in the  $g$  value of the conduction electron. Then, in theoretical evaluation for the conduction  $g$  tensor, the momentum matrix elements involved can be obtained from the effective mass and the spin-orbit matrix element from the measured splitting of the valence band, or the atomic spin-orbit splitting. Also, the energy gap involved may sometimes be obtained from optical data. In this way, agreement between the estimated  $g$  value and the experimental one provides us with another internal consistency check of the one electron theory. Although Roth's calculation<sup>4</sup> along this line for  $\delta g_{11}$  in Ge gives good agreement with experiment, her calculation for Si on a two-band model is not sufficient. We shall first demonstrate this inadequacy.

Let us assume a two-band case for Si. Then, we have for the longitudinal shift

$$\delta g_{11}^{\text{Si}} = \text{Re} \frac{4}{mi} \left( \frac{1}{E_{\Delta_1} - E_{\Delta_5}} \right)^2 \times |\langle \Delta_1 | p_y | \Delta_5^y \rangle|^2 \langle \Delta_5^y | h_x | \Delta_5^z \rangle. \quad (5.8)$$

From K-P's calculation only  $\Delta_5$  contributes appreciably to the electron effective mass at  $\Delta_1$ . Then the value of the momentum matrix element in (5.8) can be taken from the effective mass. The s-o matrix element has been calculated for  $\mathbf{k}_0$  in Sec. IV and the energy gap can be taken from K-P's band calculation. If we take  $(m/m_i^*)_{\text{Si}} = 5.2$ ,<sup>25</sup>  $E_{\Delta_1} - E_{\Delta_5} = 4.7$  eV,<sup>17</sup> and  $\Delta_{\text{s-o}} = 0.0011$  eV from (4.12), the magnitude of  $\delta g_{11}$  is evaluated to be  $0.98 \times 10^{-3}$ . Next we consider the question of *sign*. From (5.8) we see that the sign of  $\delta g_{11}$  is determined by the sign of  $(1/i) \langle \Delta_5^y | h_x | \Delta_5^z \rangle$ , which can be related to the atomic core s-o matrix element by

$$(1/i) \langle \Delta_5^y | h_x | \Delta_5^z \rangle = (|b_{2p'}^{\Delta_5}|^2 - |b_{2p}^{\Delta_5}|^2) (1/i) \langle \chi_y | h_x | \chi_z \rangle. \quad (5.9)$$

From (4.4) and the fact that the quartic-degenerate state, which corresponds to an atomic  $P_{3/2}$  state, lies above the doubly degenerate one at  $\Gamma$ , it is readily established that the sign of  $(1/i) \langle \chi_y | h_x | \chi_z \rangle$  is negative. Furthermore, from the discussion of s-o splitting and specifically from (4.9) and (4.11), we see that  $|b_{2p'}^{\Delta_5}| < |b_{2p}^{\Delta_5}|$  at  $\mathbf{k}_0$ . Then according to (5.8),  $\delta g_{11}^{\text{Si}}$  has a positive sign. The question of sign for  $\delta g_{11}^{\text{Si}}$  was first pointed out by Yafet.<sup>26</sup> A rough estimate for  $\delta g_{11}^{\text{Si}}$  in the two-band case gives it a negative value, the magnitude of which is one fifth of that of  $\delta g_{11}$ .

In short, assuming a two-band case for Si, the calculated values for the conduction  $g$  tensor do not show any agreement with the experimental values<sup>27</sup> which not only give a negative  $\delta g_{11}$  but also a  $\delta g_{11}$  larger

<sup>23</sup> H. R. Philipp and E. A. Taft, Phys. Rev. **113**, 1002 (1959).

<sup>24</sup> R. N. Dexter, H. J. Zeiger, and B. Lax, Phys. Rev. **104**, 637 (1956).

<sup>25</sup> C. J. Rauch, J. J. Strickler, H. J. Zeiger, and G. S. Heller, Phys. Rev. Letters **4**, 64 (1960).

<sup>26</sup> Y. Yafet (private communication).

<sup>27</sup> D. K. Wilson and G. Feher, Phys. Rev. **124**, 1068 (1961).

in magnitude than  $\delta g_{11}$ . For Ge, however, a two-band calculation gives a negative  $\delta g_{11}$  consistent with experiment. This reversal in sign from Si to Ge is reflected in the s-o split levels for the valence band by the cross-over along  $\Delta_3$  discussed in Sec. IV.

### Calculation of $g$ Tensor

From the failure of a two-band approximation, we see that the problem of  $g$  tensor in Si is complicated. It is not possible to evaluate the shift purely from experimental parameters. For Si, we use K-P wave functions to calculate some of the matrix elements involved. First of all, because of the selection rule  $\langle X_4^n | h | X_4^n \rangle = 0$ , we expect that the largest contribution comes from the interband s-o matrix element  $\langle \Delta_5^n | h | \Delta_5^{n'} \rangle \sim \langle X_4^n | h | X_4^{n'} \rangle$ .<sup>23</sup> It is found that the most important terms in the  $g$  shift for Si involve matrix elements of this form when one of the levels involved belongs to the  $2p$  core state, which is far below the conduction band. The reason that such a low-lying state can make important contributions to the  $g$  shift is due to the small magnitude of the s-o splitting of the valence  $\Delta_5$  state at  $\mathbf{k}_0$ , which we have calculated in Sec. IV. Therefore, the gain in s-o matrix element by going to the  $2p$  core, even after being offset by the loss due to the energy denominator, still gives dominating contributions. In the calculation of the momentum matrix element between valence states, we follow the discussion in effective-mass evaluation and use the plane-wave part of the crystal wave function. In the evaluation of the momentum matrix element involving core states, we use the Slater type analytic wave functions for the core used by Woodruff.<sup>29</sup> See Table II for the relative importance of different

TABLE II. Relative magnitude of contributions to  $g$  tensor in Si.<sup>a</sup>

Term in (5.2) involving:			Relative magnitude with respect to first term in $\delta g_{11}^{\text{Si}}$
$\delta g_{11}$	$\langle \Delta_1   p_y   \Delta_5^y \rangle$	$\langle \Delta_5^y   h_x   \Delta_5^z \rangle$	1
	$\langle \Delta_1   p_y   \Delta_5^{1y} \rangle$	$\langle \Delta_5^{1y}   h_x   \Delta_5^z \rangle$	0.7
	$\langle \Delta_1   p_y   \Delta_5^y \rangle$	$\langle \Delta_5^y   h_x   \Delta_5^{1z} \rangle$	0.7
	$\langle \Delta_1   p_y   \Delta_5^{1y} \rangle$	$\langle \Delta_5^{1y}   h_x   \Delta_5^z \rangle$	-2.6
	$\langle \Delta_1   p_y   \Delta_5^y \rangle$	$\langle \Delta_5^y   h_x   \Delta_5^{1z} \rangle$	-2.6
$\delta g_{12}$	$\langle \Delta_1   p_z   \Delta_5^z \rangle$	$\langle \Delta_5^z   h_y   \Delta_5^z \rangle$	-0.5
	$\langle \Delta_1   p_z   \Delta_5^z \rangle$	$\langle \Delta_5^z   h_y   \Delta_1^1 \rangle$	0.3
	$\langle \Delta_1   p_z   \Delta_5^{1z} \rangle$	$\langle \Delta_5^{1z}   h_y   \Delta_1^1 \rangle$	-0.2
	$\langle \Delta_1   p_z   \Delta_5^z \rangle$	$\langle \Delta_5^z   h_y   \Delta_1^1 \rangle$	-3.1
	$\langle \Delta_1   p_z   \Delta_5^{1z} \rangle$	$\langle \Delta_5^{1z}   h_y   \Delta_1^1 \rangle$	-0.3

<sup>a</sup> The first term in  $\delta g_{11}$  is the only one contributing in the two-band approximation.

<sup>23</sup> The first important observation of the effect of a matrix element like this was in the intensity ratio of the  $^2P-^2S$  doublet by Fermi [E. Fermi, Z. Physik **59**, 680 (1929)]; also see E. U. Condon and G. Shortley, *Theory of Atomic Spectra* (Cambridge University Press, New York, 1953), p. 376.]

<sup>29</sup> T. O. Woodruff, Phys. Rev. **103**, 1159 (1956).

terms in calculating the Si  $g$  tensor. The calculated results for  $\delta g_{11}^{\text{Si}}$  and  $\delta g_{12}^{\text{Si}}$  are listed in Table III together with their experimental values by Wilson and Feher.<sup>27</sup>

After the investigation for Si, we come to ask ourselves whether a two-band approximation is sufficient for Ge, especially, what is the role of the various core states involved. For this investigation, we use our own Ge crystal wave function. We do not want to consider any term in Eq. (5.3) which contains core states twice (these are very small because of the square of a large energy denominator involved). So we have to mix one of the valence states to the conduction state by a momentum operator and then mix this valence state to one of the core states by the s-o operator in order to get any appreciable contribution to the  $g$  tensor. Since we have seen in the previous section that there is largely  $3p$  character in the valence states involved, we need only consider the  $3p$  core state. Investigation along this line shows that the core contributions to both  $\delta g_{11}^{\text{Ge}}$  and  $\delta g_{12}^{\text{Ge}}$  are negligible. Then, a two-band approximation ( $L_1$  and  $L_3$  states in Fig. 2) should be sufficient for  $\delta g_{11}^{\text{Ge}}$ . For  $\delta g_{12}^{\text{Ge}}$  the most important contribution comes from the first term in the appropriate formula in (5.3) when the three bands involved are  $L_1$ ,  $L_3$ , and  $L_3'$  of Fig. 2. The contribution from other terms is very small. In particular  $\Delta g_{12}'$  in Roth's<sup>4</sup> original notation amounts only to 1% of the most important term: This verifies Phillip's conjecture as mentioned in Roth's paper. Since there are very few bands involved, we can use the experimental values for the effective mass and the s-o splitting in the calculation of conduction  $g$  tensor whenever this is applicable. The calculated values are listed in Table III.

It is to be noticed that the calculated value for  $\delta g_{12}$  has the right magnitude but the wrong sign as compared with the experimental one by Wilson and Feher.<sup>30</sup> Several possible causes for this discrepancy may be mentioned. The one-electron approximation and the effective-mass formalism have been tested in many ways in other experiments and in the other parameters calculated here, with good agreement between experiment and theory. The present calculation is rather insensitive to the band structure because the most important energy denominator  $E_{L_1} - E_{L_3'}$  is taken from experiment, and because the momentum matrix elements are close to those of nearly free-electron wave functions. Further there is no selection rule for the s-o

TABLE III.  $g$ -tensor.

		$\delta g_{11}$	$\delta g_{12}$
Si	Calc.	-0.0027	-0.0036
	Exp.	-0.0028	-0.0040
Ge	Calc.	-1.0	+0.069
	Exp.	-1.13	-0.082

<sup>30</sup> D. K. Wilson and G. Feher, Bull. Am. Phys. Soc. **5**, 60 (1960).

matrix elements, which are normal. It therefore appears most likely that an error in sign has been made. A careful search has been made, but with no success.

## VI. SPIN-LATTICE RELAXATION IN Si

Roth<sup>9</sup> has proposed a spin-lattice relaxation mechanism for donor electrons in Si, which is the whole relaxation mechanism when the magnetic field is in the [100] direction ( $x$  direction). This mechanism, according to Roth, arises from the interaction which is responsible for the modulation of the single valley  $g$ -tensor values when the crystal is under uniaxial stress along the [111] direction. The interaction takes the following form:

$$\mathcal{H} = A(\beta/2)\{\epsilon_{yz}(\sigma_y H_z + \sigma_z H_y) + \text{cycl. perm.}\}, \quad (6.1)$$

where  $\beta$  is the Bohr magneton and  $\epsilon_{yz}$  is the  $yz$  component of the strain tensor. When the Si sample is put under stress in the [111] direction, the  $\Delta_{2'}$  state which is very close to the  $\Delta_1$  conduction band edge gets mixed into  $\Delta_1$  through the shear deformation potential component  $E_{yz}$  if the effect of crystal deformation on the electronic states is treated by perturbation theory. Roth argued that in view of the small energy gap between  $\Delta_1$  and  $\Delta_{2'}$  at the band edge (0.35 eV according to our calculation), the most important terms in the parameter  $A$  should involve  $\Delta_{2'}$  at least twice and are equal to

$$A = \frac{4i}{3m} \frac{\langle \Delta_{2'} | p_x | \Delta_{2'} \rangle \langle \Delta_{2'} | E_{yz} | \Delta_1 \rangle}{E_{12'}^2 E_{15}} \times \{ \langle \Delta_1 | p_y | \Delta_5^y \rangle \langle \Delta_5^y | h_y | \Delta_{2'} \rangle + \langle \Delta_1 | h_y | \Delta_5^z \rangle \langle \Delta_5^z | p_y | \Delta_{2'} \rangle \}. \quad (6.2)$$

We have investigated all the remaining terms in the perturbation expansion for  $A$ , paying particular attention to the core states and we have estimated that their net contribution amounts to no more than 10% of the two terms already listed in (6.2). Wilson and Feher<sup>27</sup> in their experiments measured the change in the conduction  $g$  value when the Si sample is put under stress along the [111] direction and hence the parameter  $A$ . On the other hand, we have calculated all the  $s$ - $o$  and momentum matrix elements and energy-gap values

involved in  $A$ . Using their experimental value of  $A = 0.44 \pm 0.04$ , we then get a value of 23 eV for  $\langle \Delta_{2'} | E_{yz} | \Delta_1 \rangle$ . This is to be compared with the intra-band shear deformation potential matrix element  $E_2 = \langle \Delta_1 | E_{yy} | \Delta_1 \rangle = 7$  eV from conductivity measurements.<sup>31</sup>

Wilson and Feher<sup>27</sup> also measured the relaxation rate due to the mechanism in (6.1) and compared the experimental value with the value obtained by theoretical formula after putting  $A = 0.44$  from the measurement of shift in  $g$  value due to strain. They found that the theoretical relaxation rate is too slow by about a factor of 2. In other words, if we are to estimate  $A$  from the relaxation rate measurement, assuming the proposed mechanism, we would get a value for  $A$  two times larger than 0.44. This in turn would give a value for  $\langle \Delta_{2'} | E_{yz} | \Delta_1 \rangle$  two times larger than what we have estimated.

Roth<sup>9</sup> and Hasegawa<sup>10</sup> have independently proposed another mechanism for the donor spin-lattice relaxation in Si, which is caused by the change in  $g$  value due to valley repopulation and depends primarily on  $g_{11} - g_{\perp}$ . Wilson and Feher<sup>27</sup> in their experiment also measured the relaxation rate due to this mechanism. Using their measured value, Yafet<sup>26</sup> then estimated  $E_2$  involved to be 20 eV. Comparison of this value with 7 eV from conductivity measurements gives us an idea about the range of error we should expect by estimating deformation potentials from spin-lattice relaxation measurements.

## APPENDIX. BAND CALCULATION FOR Ge

A band calculation for Ge is done by the orthogonalized plane wave method. The crystal potential is assumed to be composed of two parts, Coulomb part and exchange part. For the Coulomb potential a superposition of atomic charge distribution is assumed. The atomic H-F wave function for Ge is furnished by Piper. For the exchange potential we adopt Slater's approximation

$$V^{\text{ex}}(\mathbf{r}) = -6[(3/8\pi)\rho(\mathbf{r})]^{1/2}, \quad (A1)$$

lumping both core and valence charge densities together. The valence wave function is orthogonalized to atomic-core wave function and the orthogonalization coefficients  $A_i$  are listed in Table IV. Note that the

TABLE IV. Orthogonalization coefficients for Ge.

$ \mathbf{k} + \mathbf{K} ^2$	$A_{1s}$	$A_{2s}$	$A_{3s}$	$-iA_{2p}$	$-iA_{3p}$	$A_{3d}$
0	0.00469	-0.03287	0.15285	0.00000	0.00000	0.00000
3	0.00468	-0.03193	0.12669	0.00560	-0.08660	0.06560
4	0.00468	-0.03167	0.11920	0.00641	-0.09390	0.07652
8	0.00467	-0.03066	0.09385	0.00878	-0.10505	0.09717
11	0.00466	-0.02994	0.07872	0.01006	-0.10479	0.10091
12	0.00467	-0.02970	0.07427	0.01043	-0.10393	0.10109
16	0.00464	-0.02879	0.05892	0.01169	-0.09848	0.09896
19	0.00463	-0.02813	0.04952	0.01246	-0.09330	0.09574

<sup>31</sup> R. W. Keyes, *Solid State Physics*, edited by F. Seitz and D. Turnbull (Academic Press, Inc., New York, 1960), Vol. 2.

TABLE V. Energy eigenvalues for Ge (in ry).

$\Gamma_1$	$L_{2'}$	$L_1^1$	$L_{3'}$	$\Gamma_{25'}$	$L_1$	$\Gamma_{15}$	$\Gamma_{2'}$	$L_3$	$L_{2'}^1$
-1.924	-1.704	-1.523	-1.172	-1.036	-0.824	-0.792	-0.765	-0.730	-0.478

orthogonalization coefficients  $B_t$  in all the formulas related to the s-o splitting in this paper differ from the listed  $A_t$  by a factor of  $\sqrt{2}$  ( $B_t = \sqrt{2}A_t$ ). This is because there are two atoms per unit cell for diamond structure and we have included a  $1/\sqrt{2}$  factor in the core function  $\phi_{k,t}^\alpha$  in (3.2) to have it properly normalized. By taking  $V_{000} = -2.58$  ry according to F. Herman [Physica **20**, 801 (1954)], we have obtained the energy eigenvalues (Table V) and eigenvectors for states at  $\Gamma$  and  $L$ . The energy bands thus obtained agree qualitatively with a similar calculation by Herman, except that our calculation gives a  $\Gamma_{15}$  state lower than  $\Gamma_{2'}$  state in energy,

in contradiction with both Herman's calculation and experiment. However, an adjustment of the value for  $V_{000}$  can bring down  $\Gamma_{2'}$  relative to  $\Gamma_{15}$  state, and produce a value for the conduction-valence gap at  $\Gamma$  and  $L$  in agreement with experiment. For the most crucial gap value  $E_{L_1} - E_{L_3'}$  in our  $g$ -tensor calculation we have used experimental value. Moreover, the calculated crystal band s-o splitting value depends primarily on the magnitude of the orthogonalization coefficients, the accuracy of which depends on that of H-F atomic-core wave function. The plane-wave coefficients are not even sensitive to band calculations for different substances of the same crystal structure. For example, comparing the Si result by K-P and the Ge result by us, we often find agreement to at least the first figure between the corresponding plane-wave coefficients for some of the important states. Therefore, no attempt has been made to recalculate the eigenvalues and eigenvectors with different choices of  $V_{000}$ . The calculated values for the plane-wave coefficients for various states of Ge are contained in Table VI.

#### ACKNOWLEDGMENTS

The author wishes to express his gratitude to Professor J. C. Phillips for suggesting the problem and many helpful comments, and to Professor M. H. Cohen for interesting discussions. He is also indebted to Dr. O. C. Simpson for his hospitality at Argonne and to Dr. F. Bassani, and M. Yoshimine for discussions and for allowing him to use their computer program for OPW band calculation. The atomic H-F wave function for Ge was furnished by Dr. W. W. Piper prior to publication, to whom the author extends his deep gratitude.

TABLE VI. Plane-wave coefficients for Ge.

$(\mathbf{k}+\mathbf{K})$	$\Gamma_1$	$\Gamma_{25'}$	$\Gamma_{2'}$	$\Gamma_{15}$		
(000)	0.977					
(111)	-0.361	0.796	0.974	0.990		
(200)		0.669	0.536			
(220)	0.007	-0.006		0.316		
(311) <sub>1</sub>	0.061	-0.148	0.099	0.113		
(311) <sub>2</sub>		-0.073		0.110		
(222)	0.018	-0.094	0.076	0.026		
(400)	0.038			0.020		
(331) <sub>1</sub>	-0.037	-0.006				
(331) <sub>2</sub>			0.068	-0.014		
$L_{2'}$	$L_1^1$	$L_{3'}$	$L_1$	$L_3$	$L_{2'}^1$	
$(\frac{1}{2} \frac{1}{2} \frac{1}{2})$	1.013	0.946		0.190	-0.178	
$(\frac{3}{2} \frac{1}{2} \frac{1}{2})$	-0.217	0.346	1.002	-1.054	0.820	-0.945
$(\frac{5}{2} \frac{1}{2} \frac{1}{2})$	0.160	0.249	-0.149	0.286	-0.503	-0.085
$(\frac{7}{2} \frac{1}{2} \frac{1}{2})$	-0.033	0.025	0.188	0.089	0.110	-0.263
$(\frac{9}{2} \frac{1}{2} \frac{1}{2})$	0.123	-0.127		-0.025		-0.119
$(\frac{11}{2} \frac{1}{2} \frac{1}{2})_1$	-0.097	0.047	0.085	0.022	-0.254	0.049
$(\frac{11}{2} \frac{1}{2} \frac{1}{2})_2$			0.134		-0.405	
$(\frac{13}{2} \frac{1}{2} \frac{1}{2})$	-0.058	-0.034	0.128	0.058	-0.106	-0.074
$(\frac{15}{2} \frac{1}{2} \frac{1}{2})$	-0.042	-0.054	-0.004	-0.042	0.043	-0.009
$(\frac{17}{2} \frac{1}{2} \frac{1}{2})$	0.070	0.034		-0.030		0.041